Submitted to

33rd International Conference on High Energy Physics, ICHEP06, July-August, 2006, Moscow
Abstract:
Parallel Session **Hadron Spectroscopy and Exotics**

www-h1.desy.de/h1/www/publications/conf/conf_list.html

Search for Baryonic States Decaying to $\Xi\pi$ in Deep Inelastic Scattering at HERA

H1 Collaboration

Abstract

A search for narrow baryonic states decaying into $\Xi^-\pi^-$ or $\Xi^-\pi^+$ and their antiparticles is carried out with the H1 detector using deep inelastic scattering events at HERA, at centre-of-mass energies of 300 and 318 GeV. No signal is observed for a new baryonic state in the mass range 1600 - 2100 MeV in neither the $\Xi^-\pi^-$ nor the $\Xi^-\pi^+$ decay channels. The standard baryon $\Xi(1530)^0$ is observed through the decay mode $\Xi(1530)^0 \to \Xi^-\pi^+$. Upper limits on the ratio of the hypothetical pentaquark states Ξ_{5q}^{--} and Ξ_{5q}^{0} to the $\Xi(1530)^0$ signal are given.

1 Introduction

Various experiments have reported evidence for narrow signals with masses around 1520 MeV, decaying into nK^+ and pK^0_S final states [1]. Such states could be interpreted as an exotic strange pentaquark baryon state with a minimal quark content of $uudd\bar{s}$. On the other hand, a number of other experiments have reported negative evidence for the same state.

Such states are expected to occur as a flavour antidecuplet within various theoretical approaches using QCD [2]. The state reported above is referred to as the Θ^+ [1]. Searches for the other members of this decuplet are of interest, in particular the doubly strange Ξ^{--}_{5q} $(ddss\bar{u})$ and Ξ^{+}_{5q} $(uuss\bar{d})$ states, which are manifestly exotic. However, states from the standard isospin $3/2$ baryon multiplet such as the Ξ^0 and the Ξ^- can also populate states similar to these pentaquark states

The NA49 [3] collaboration reported the observation of the Ξ^{--}_{5q} and Ξ^{0}_{5q} members of the $\Xi_{3/2}$ multiplet, with a mass of $1862 \pm 2\,\mathrm{MeV}$ and a width of less than $18\,\mathrm{MeV}$. These findings have not been confirmed by several other experiments [4], including the ZEUS collaboration [5].

This analysis describes results of a search for such new baryonic states decaying into the $\Xi^-\pi^\pm$ and $\Xi^+\pi^\pm$ final states. The $\Xi^-(\Xi^+)$ particles were identified through their decay channels into $\Lambda\pi^-(\bar{\Lambda}\pi^+)$. This search is performed using $102.5\,\mathrm{pb}^{-1}$ of deep inelastic ep scattering data taken with the H1 detector in the years 1996 - 2000.

2 Experimental Procedure

2.1 H1 Apparatus

In the following only those detector components important for the present analysis are described. A detailed description of the H1 detector can be found in [6].

The tracks from charged particles used in this analysis are reconstructed in the central tracker, whose main components are two cylindrical drift chambers, the inner and outer central jet chamber (CJCs) [7]. The inner and outer CJC are mounted concentrically around the beam-line, covering the range of pseudorapidities[2] $-1.75 < \eta < 1.75$ for tracks coming from the nominal event vertex. The CJCs lie within a homogeneous magnetic field of $1.15\,\mathrm{T}$ which allows the transverse momentum, p_{T}, of charged particles to be measured. Two additional drift chambers complement the CJCs by precisely measuring the z coordinates of track segments and hence assist in the determination of polar angles. Two cylindrical multi-wire proportional chambers facilitate triggering on tracks. The transverse momentum resolution of the central tracker is $\sigma(p_{\mathrm{T}})/p_{\mathrm{T}} \simeq 0.005\,p_{\mathrm{T}}\ /\ \mathrm{GeV} \oplus 0.015$. Charge misidentification is negligible for particles originating from the primary vertex and having transverse momenta in the range relevant to this analysis.

[1]Unless explicitely mentioned, the charge conjugate states are always implicitly included.

[2]The pseudorapidity is given by $\eta = -\ln\tan\theta/2$, where the polar angle θ is measured with respect to the z axis given by the proton beam direction.

The backward region of H1 is equipped with a lead/scintillating fibre "Spaghetti" Calorimeter (SpaCal) [8], which is optimized for the detection of the scattered positron in the DIS kinematic range considered here. It consists of an electromagnetic and a more coarsely segmented hadronic section. A planar drift chamber, positioned in front of the SpaCal, improves the measurement of the polar angle, and is used to reject neutral particle background. The global properties of the hadronic final state are reconstructed using an algorithm which combines information from the central tracker, the SpaCal and the Liquid Argon calorimeter, which surrounds the central tracker. The DIS events studied in this paper are triggered on the basis of an energy deposition detected in the SpaCal, complemented by signals in the CJCs and the multi-wire proportional chambers in the central tracker.

The luminosity measurement is based on the Bethe-Heitler process $ep \rightarrow ep\gamma$, where the photon is detected in a calorimeter located downstream of the interaction point.

2.2 Simulation of Baryonic states

To estimate the acceptance, the efficiency and the resolution for the detection of a hypothetical baryon state, a Monte Carlo simulation based on the PYTHIA 6.2 [9] event generator is used, incorporating the Lund string model of fragmentation [10]. The kinematic distributions of strange baryons in DIS data have been found to be reasonably well described [11] by the PYTHIA simulation. The Ξ^{--}_{5q} state is introduced by changing the mass of the standard Δ^{--} antibaryon to values in the required ranges from 1.6 to 2.1 GeV and forcing it to decay into $\Xi\pi$ final states. Due to lack of knowledge of the pentaquark production mechanism, it is assumed that the production kinematics of the Ξ^{--}_{5q} is similar to those of other baryons and that it decays isotropically. In the simulation, the Ξ^{--}_{5q} particle is produced on mass shell. The generated events are passed through the standard H1 detector simulation based on GEANT [12] and then through the identical reconstruction and analysis chain as the data.

2.3 Selection of DIS Events

The analysis is carried out using data corresponding to an integrated luminosity of $\mathcal{L} = 102.5\,\mathrm{pb}^{-1}$, taken in the years 1996 - 2000. During this time HERA collided electrons[3] at an energy of $27.6\,\mathrm{GeV}$ with protons at $820\,\mathrm{GeV}$ (1996 - 1997) and $920\,\mathrm{GeV}$ (1999 - 2000)[4].

Events are selected if the z coordinate of the event vertex, reconstructed using the central tracker, lies within $35\,\mathrm{cm}$ of the mean position for ep interactions. The scattered electron is required to be reconstructed in the SpaCal with an energy, E'_e, above $8\,\mathrm{GeV}$. The negative four momentum transfer squared of the exchanged virtual photon, Q^2, is required to lie in the range $2\,\mathrm{GeV}^2 < \mathrm{Q}^2 < 120\,\mathrm{GeV}^2$, as reconstructed from the energy and polar angle of the scattered electron. The inelasticity y of the event is reconstructed using the scattered electron kinematics and is required to be in the range $0.05 < y < 0.7$. The difference between the total energy E and the longitudinal component of the total momentum p_z, calculated from the electron and the

[3]The analysis uses data from periods when the beam lepton was either a positron or an electron.

[4]The sample with a proton energy of $820\,(920)$ GeV corresponds to a luminosity of $\mathcal{L} = 26.8\,(75.7)\,\mathrm{pb}^{-1}$.

hadronic final state, is restricted to $35\,\mathrm{GeV} < \mathrm{E} - \mathrm{p_z} < 70\,\mathrm{GeV}$. This requirement suppresses photoproduction background, in which the electron escapes detection and a hadron fakes the electron signature.

2.4 Selection of the Baryon Candidates

The identification of the baryon states is done by the complete reconstruction of their decay chain through Ξ and Λ baryons into pions and protons:

$$\Xi^{--} \rightarrow \Xi^-\pi^- \rightarrow (\Lambda\pi^-)\pi^- \rightarrow [(p\pi^-)\pi^-]\pi^- \quad (1)$$

The decay daughter particles are fitted in 3 dimensions to their respective decay vertices [13], which are referred to as the tertiary (Λ-decay) and the secondary (Ξ-decay) vertex. The analysis is based on charged particles reconstructed in the central tracker. If not mentioned otherwise, tracks are accepted if they have transverse momenta $p_{\mathrm{T}} > 0.12\,\mathrm{GeV}$ and pseudorapidity $|\eta| < 1.75$.

In the first step, the Λ baryons are identified by their charged decay mode, $\Lambda \rightarrow p\pi^-$, using pairs of oppositely charged tracks, assuming a proton and pion hypothesis, respectively. The track with the higher momentum is assigned the proton mass. The particles are fitted to a tertiary vertex and required to have a vertex fit probability above 1% and a 2-dim decay length (in the $r - \phi$ plane) larger $7.5\,\mathrm{mm}$. The Λ transverse momentum is required to be $p_T > 0.3\,\mathrm{GeV}$. The potential contamination from $K^0_S \rightarrow \pi^+\pi^-$ is rejected by a cut on the $\pi\pi$ invariant mass of $\pm 10\,\mathrm{MeV}$ around the nominal K^0_S mass. The resulting invariant-mass spectra for $p\pi^-$ and $\bar{p}\pi^+$ are shown in Fig. 1.

In the second step, Ξ^- candidates are formed by fitting the Λ candidates, taken within $\pm$ $8\,\mathrm{MeV}$ of the nominal Λ mass, with negatively charged tracks to a secondary vertex. Ξ^- candidates are retained if the vertex fit probability is above 1% and the 2-dim distance of closest approach (DCA) of the Ξ track was smaller than 2.5 mm with respect to the primary vertex. To increase the significance of the Ξ^- signal it is required that the angle between the secondary and the tertiary vertex vectors be less than 0.6 rad. For the Ξ candidate combinations, passing these criteria, the invariant-mass spectra $\Lambda\pi^-$ and $\bar{\Lambda}\pi^+$ are shown in Fig. 2.

In the third step, the Ξ^- candidates within $\pm 15\,\mathrm{MeV}$ of the nominal Ξ mass are selected and combined with candidate $\pi^\pm$ tracks. The π tracks are required to originate from the primary vertex and to have a significance(DCA/σ_{DCA}) to the primary vertex of less than 4. To reduce the background further, the transverse momentum of the $\Xi\pi$ combination is required to be $> 1.0\,\mathrm{GeV}$. These $\Xi^\pm\pi^\pm$ and $\Xi^\pm\pi^\mp$ combinations are investigated further in section 3.

3 Resulting Spectra and Limit Calculation

The resulting invariant-mass spectra for each of the four charge combinations $\Xi^-\pi^-$, $\Xi^-\pi^+$, $\Xi^+\pi^-$, $\Xi^+\pi^+$ are shown in Fig. 3a,b,d,e separately. The sum of the equal charge ($++$ and $--$) and opposite charge ($+-$ and $-+$) combinations are also shown in Fig. 3c and f. In both the

$\Xi^-\pi^+$ and $\Xi^+\pi^-$ (Fig. 3a,b spectra, and correspondingly in the Fig. 3c), the signal of the well known $\Xi(1530)^0$ state [14] is clearly observed. A fit of the data (Fig. 3c) with a Gaussian for the signal and background is made using,

$$B(M) = P_1(M - m_\Xi - m_\pi)^{P_2} \times (P_3 + P_4 M + P_5 M^2), \tag{2}$$

where M is the $\Xi\pi$ invariant mass, m_Ξ and m_π are the masses of the Ξ and the π, respectively, and P_i are free parameters.

The fit yields a total of $170\ \pm\ 28\,(stat.)$ $\Xi(1530)^0$ baryons. The reconstructed mass of $1530\ \pm\ 2\,(stat.)\,\mathrm{MeV}$ is consistent with the PDG value [14]. The measured width of $8.9\ \pm$ $1.3(stat.)\,\mathrm{MeV}$ is consistent with the detector resolution, and is also correctly described by the simulations.

Figure 4 shows the sum of the invariant mass spectra for equal and opposite charge ($+-$ and $-+$ and $--$ and $++$) combinations for events having Q^2 larger than $20\,\mathrm{GeV}^2$. The ZEUS collaboration reported to have seen a hint for a structure around $1690\,\mathrm{MeV}$ representing the $\Xi(1690)^0$ baryonic state [5]. In this analysis there is no hint for such a structure observed.

The ratio of the equal to opposite charge mass spectra (Fig. 3c divided by Fig. 3f), is shown in Fig.5. It appears to be reasonably flat in the mass region above the $\Xi(1530)^0$. This supports the use of the same background shape function for both charge combinations and indicates that the reconstruction efficiencies are very similar.

No signal is observed near $1860\,\mathrm{MeV}$ in any of the equal charge mass spectra (Fig. 3a,b) nor in the opposite charge ones (Fig. 3d,e). Therefore, upper limits are set on the production of new states decaying to $\Xi^-\pi^-$ in the mass range 1.6 - 2.1 GeV in the kinematic region $0.05 < y < 0.7$ for $2\,\mathrm{GeV}^2 < \mathrm{Q}^2 < 120\,\mathrm{GeV}^2$. To quantify such limits the ratio R(M) is determined using

$$R_{u.l.}(M) = \frac{\frac{dN_{u.l.}}{dM}(\Xi^\pm\,\pi^\pm)}{N(\Xi(1530)^0)}, \tag{3}$$

where M is the $\Xi\pi$ invariant mass and $N(\Xi(1530)^0)$ represents the number of $\Xi(1530)^0$ states, measured in the data with the same kinematic conditions. This ratio is presumed to be sensitive to the existence of new states, because of the clean signal observed for the established $\Xi(1530)^0$. The ratio also has the advantage that the systematic effects of the acceptances and the reconstruction efficiencies mostly cancel, making it insensitive to detector effects and thus provides a robust method for the limit determination.

An upper limit at the 95% confidence level (C.L.) on $R_{u.l.}(M)$ is obtained from the observed spectra using a modified frequentist approach based on likelihood ratios [15]. This method takes the statistical and systematic uncertainties in the number of signal and background combinations into account. The M(Ξ_{5q}^{--}) distribution for signal combinations is assumed to be a Gaussian with a mean M and a width corresponding to the experimental mass resolution as obtained from the Monte Carlo simulations. This width $\sigma(M)$ varies from 7.5 to $18.4\,\mathrm{MeV}$ in the mass ranges from 1.6 to $2.1\,\mathrm{GeV}$ considered here. The background M distribution is modelled according to the data given by equation (2). The limit is then calculated in a sliding mass window of mass-dependent width $2\sigma(M)$ of the hypothetical particle in the mass range.

The systematic uncertainties in the number $N(M)$ of observed $\Xi^-\pi^-$ combinations due to Ξ_{5q}^{--} production comprises the following contributions:

- The uncertainty on the overall number of $\Xi(1530)^0$ candidates.
- The difference in reconstruction efficiency of the charged ($\Xi^-\pi^-$) and the neutral ($\Xi^-\pi^+$) combinations.
- The uncertainty on the width of the potential pentaquark signal.
- The uncertainty on the background distribution.
- The uncertainties due to the inclusive DIS event selection and the trigger efficiency are assumed to cancel in the ratio.

The final result of the limit calculation is shown in Figure 6, which shows in the upper part again the $\Xi\pi$ invariant-mass spectrum summed for the two equal charge combinations (upper fig., solid dots) as a function of the central value of the mass window M. In the lower part of Figure 6, the 95% C.L. upper limit on the ratio $R_{u.l.}(M)$ is given; it is found to vary from 0.15 to 0.45 in the mass range 1.6 - 2.1 GeV. In the NA49 signal region for the Ξ_{5q}^{--} candidate particle at 1.86 GeV, the ratio $R_{u.l.}(M)$ is found to be less than 0.2 at the 95% C.L.

Furthermore, no structures are observed in the opposite charge mass spectra Fig. 3c, in the mass region above the $\Xi(1530)^0$ state. Therefore, separate 95% C.L. upper limits are set on the production of new states decaying to $\Xi^-\pi^+$ or $\Xi^+\pi^-$ in the mass range 1.6 - 2.1 GeV. Figure 7 shows the resulting upper limit ratio $R_{u.l.}(M)$, which is obtained in a procedure analogous to the $\Xi^-\pi^-$ case, excluding the existence of an Ξ_{5q}^0 pentaquark state at a level ranging from 0.15 to 0.65 with respect to the $\Xi(1530)^0$ normalisation.

Finally figure 8 shows the mass spectra and 95% C.L. upper limit for all charge combinations (mass spectra in Fig. 3c and 3f summed up). In this case the upper limit $R_{u.l.}(M)$ ranges from 0.2 to 0.6.

4 Conclusion

A search for new baryonic states that decay to $\Xi^-\pi^-$ and $\Xi^-\pi^+$ and their conjugate states was performed with the H1 detector using a DIS data sample with $2 < Q^2 < 120\,\mathrm{GeV}^2$ and $0.05 < y < 0.7$, corresponding to a total integrated luminosity of $102.5\,\mathrm{pb}^{-1}$. A clear signal from the established $\Xi(1530)^0$ baryon state was seen. No pentaquark candidate signal was found and upper limits at 95% C.L. are set on the ratio of the hypothetical Ξ_{5q}^{--} and Ξ_{5q}^0 signals to the total number of observed $\Xi(1530)^0$ baryons in the mass range 1.6 to 2.1 GeV.

The results reported here are fully compatible with limits measured by the ZEUS collaboration. The overall H1 statistics in the Ξ-samples is comparable with the NA49 data. On the other hand, NA49 has a different production environment and kinematics and the limits obtained at HERA may therefore not contradict the NA49 findings.

Acknowledgements

We are grateful to the HERA machine group whose outstanding efforts have made this experiment possible. We thank the engineers and technicians for their work in constructing and maintaining the H1 detector, our funding agencies for financial support, the DESY technical staff for continual assistance and the DESY directorate for support and for the hospitality which they extend to the non DESY members of the collaboration.

References

[1] K. Hicks, Prog Part. Nucl. Phys. **55** (2005) 647 [hep-ex/0504027].
S. Chekanov *et al.* [ZEUS Collaboration], Phys. Lett. **B591** (2004) 7 [hep-ex/0403051].

[2] D. Diakonov, V. Petrov and M. Polyakov, Z. Phys. A **359**, 305 (1997) [hep-ph/9703373];
R. L. Jaffe and F. Wilczek, Phys. Rev. Lett. **91** (2003) 23 [hep-ph/0307341];
M. Karliner and H. Lipkin, Phys. Lett. **B575** (2003) 249 [hep-ph/0307243];
for a review on pentaquark phenomenology see R. L. Jaffe, Phys. Rept. **409** (2005) 1 [hep-ph/0409065].

[3] NA49 Collaboration, C. Alt *et al.*, Phys. Rev. Lett. 92 (2004) 042003 [hep-ex/0310014].

[4] WA89 Collaboration, M.I. Adamovich *et al.*, Preprint hep-ex/0405042, 2004;
ALEPH Collaboration, S. Schael *et al.*, Phys. Lett. B 599 (2004) 1;
BES Collaboration, J.Z. Bai *et al.*, Phys. Rev. D 70 (2004) 012004;
HERA-B Collaboration, I. Abt *et al.*, Phys. Rev. Lett. 93 (2004) 212003;

[5] S. Chekanov *et al.* [ZEUS Collaboration], Phys. Lett. B **610** (2005) 212 [arXiv:hep-ex/0501069].

[6] I. Abt *et al.* [H1 Collaboration], Nucl. Inst. Meth. A **386** (1997) 310;
I. Abt *et al.* [H1 Collaboration], Nucl. Inst. Meth. A **386** (1997) 348;

[7] J. Bürger *et al.*, Nucl. Instrum. Meth. A **279** (1989) 217.

[8] R. D. Appuhn *et al.* [H1 SpaCal Group], Nucl. Inst. Meth. A **386** (1997) 397;

[9] T. Sjöstrand *et al.*, Comput. Phys. Commun. **135** (2001) 238 [hep-ph/0010017].

[10] B. Andersson, G. Gustafson, G. Ingelman and T. Sjöstrand, Phys. Rept. **97** (1983) 31.

[11] M. Derrick *et al.* [ZEUS Collaboration], Z. Phys. C **68** (1995) 29 [hep-ex/9505011];
S. Aid *et al.* [H1 Collaboration], Nucl. Phys. B **480** (1996) 3 [hep-ex/9607010];
C. Risler, Ph.D. thesis, 2004, Universität Hamburg (in German), available from
http://www-h1.desy.de/publications/theses_list.html.

[12] R. Brun *et al.*, GEANT3, Technical Report CERN-DD/EE/84-1, CERN, 1987.

[13] R. Luchsinger and C. Grab, Comput. Phys. Commun. **76** (1993) 263.

[14] Particle Data Group, S. Eidelman *et al.*, Phys. Lett. **B592** (2004) 1.

[15] T. Junk, Nucl. Inst. Meth. A **434** (1999) 435 [hep-ex/9902006].

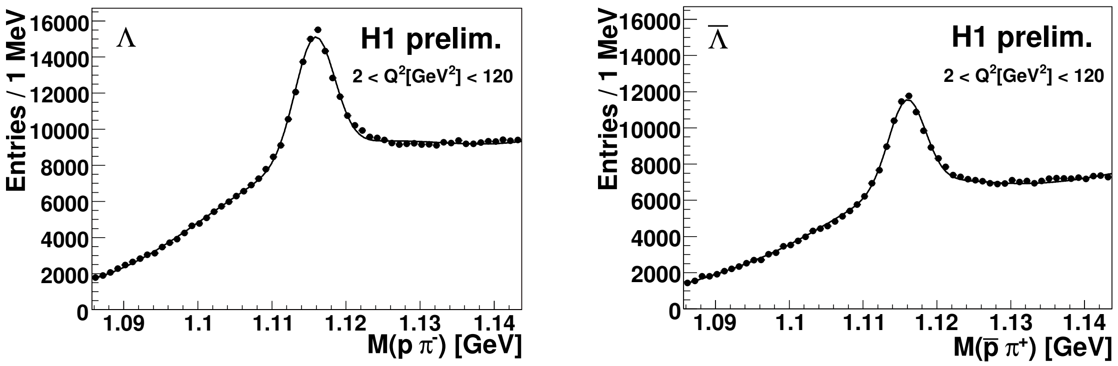

Figure 1: The invariant-mass spectra for (a) $p\pi^-$ and (b) $\bar{p}\pi^+$ combinations in the DIS kinematic region defined in the text. The solid line shows the result of a fit using a double Gaussian plus a second-order polynomial background function.

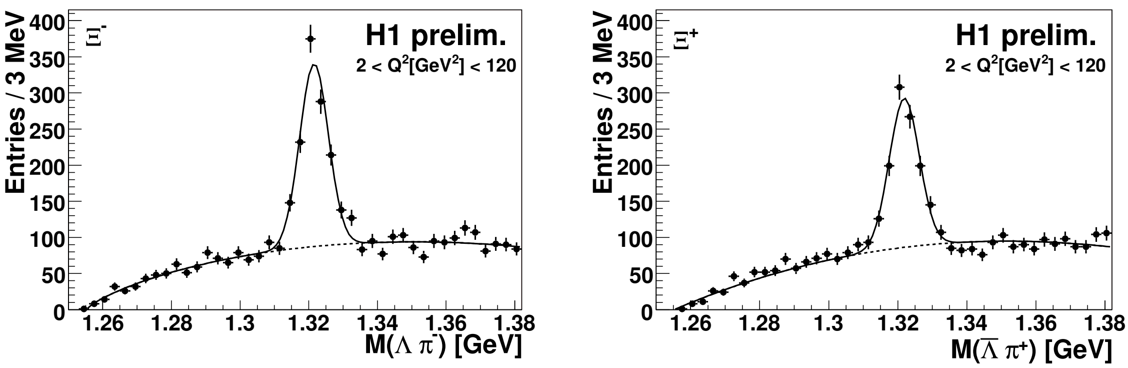

Figure 2: The invariant-mass spectra for (a) $\Lambda\pi^-$ and (b) $\bar{\Lambda}\pi^+$ particle combinations. The solid line shows the result of a fit using a Gaussian plus a background function similar to that one defined by eq. (2) , while the dashed line shows the background only.

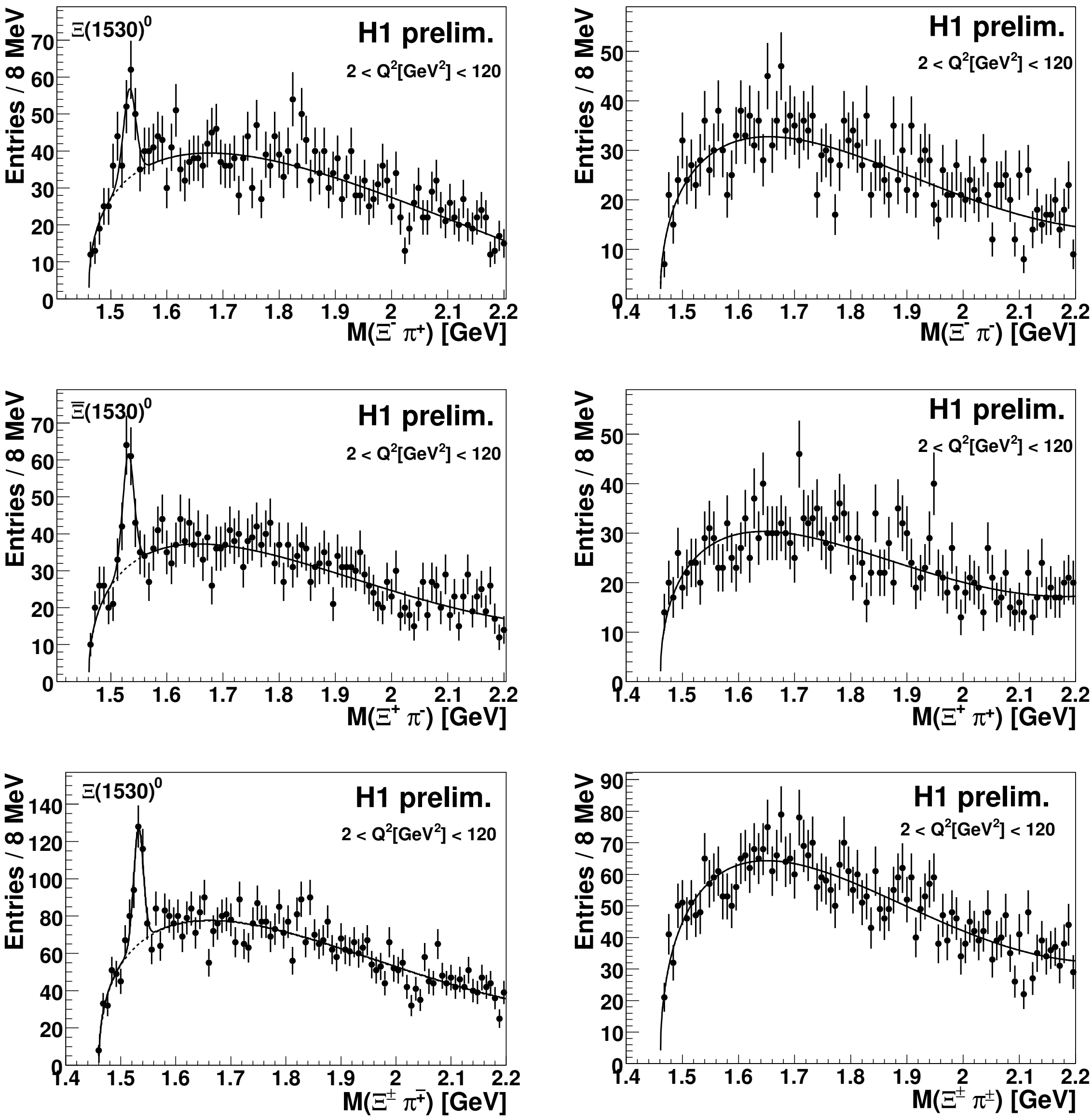

Figure 3: The invariant mass spectra of the $\Xi\pi$ particle combinations for: (left column) the opposite charge combinations $-+$, $+-$ and their sum, and (right column) equal charge combinations $--$,$++$ and their sum. The solid line in (a) is the result of a fit to the data using a Gaussian plus the background function defined by eq. (2). The dashed line shows the background according to this fit. The same background function is also shown in figures in the right column.

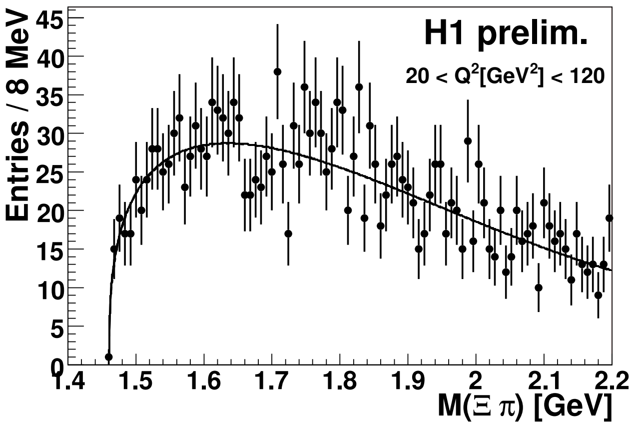

Figure 4: The invariant mass spectra of the $\Xi\pi$ particle combinations for equal and opposite charges for Q^2 larger than $20\,\mathrm{GeV}^2$. The solid line shows the result of a fit using the background function defined by eq. (2).

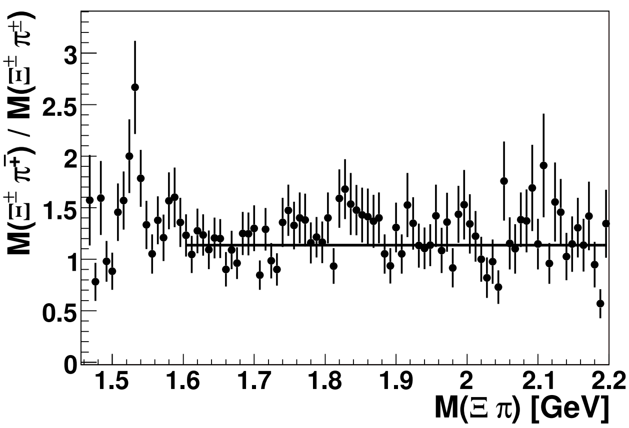

Figure 5: The ratio of the two invariant mass spectra for the opposite charge to equal charge $\Xi\pi$ combinations. The solid line is the result of a fit to the ratio, yielding a constant value of 1.13.

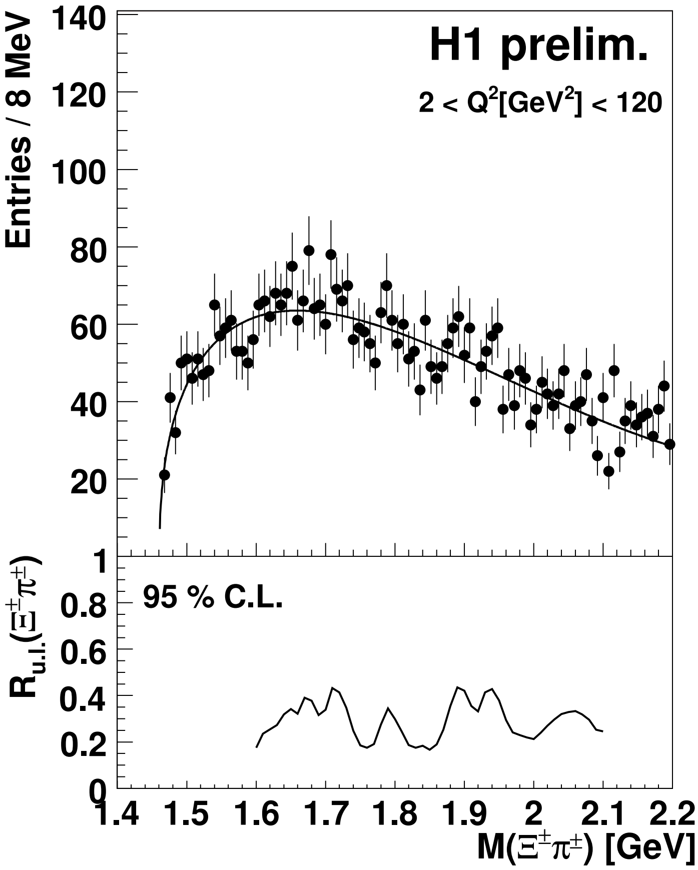

Figure 6: The $\Xi\pi$ invariant-mass spectrum summed for the two equal charge combinations (upper fig., solid dots). The solid line is the result of a fit to the data using the background function defined in eq. (2). The lower fig. shows as a function of the invariant mass the 95% C.L. upper limit on the ratio R, as defined by eq. (3).

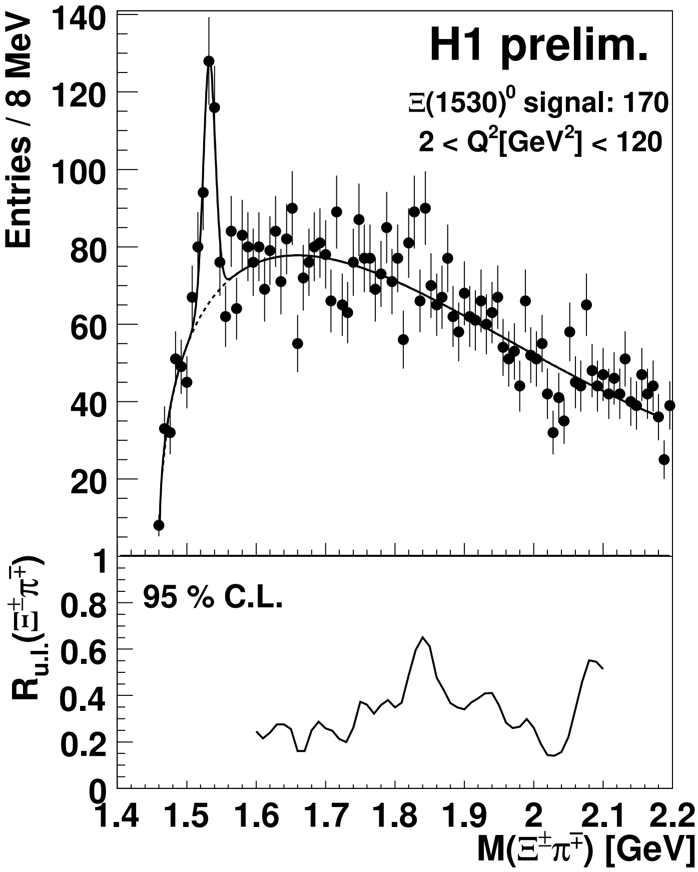

Figure 7: The $\Xi\pi$ invariant-mass spectrum summed for the two opposite charge combinations. The solid line is the result of a fit to the data using a Gaussian plus the background function defined in eq. (2). Clearly visible at a mass of 1530 MeVis the $\Xi(1530)^0$ baryon. The lower fig. shows as a function of the invariant mass the 95% C.L. upper limit on the ratio R, as defined by eq. (3).

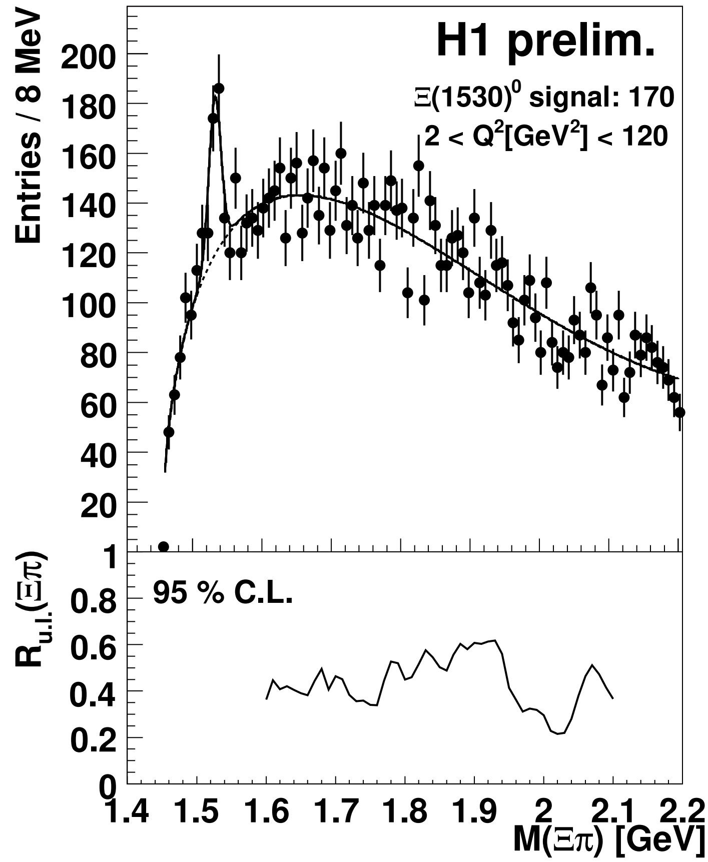

Figure 8: The $\Xi\pi$ invariant-mass spectrum summed for all charge combinations. The solid line is the result of a fit to the data using a Gaussian plus the background function defined by eq. (2). Clearly visible at a mass of $1530\,\mathrm{MeV}$ is the $\Xi(1530)^0$ baryon. The lower fig. shows as a function of the invariant mass the 95% C.L. upper limit on the ratio R, as defined by eq. (3).